A four-way coupled Euler–Lagrange approach using a variational multiscale method for simulating cavitation

Georg Hammerl, Wolfgang A. Wall

Institute for Computational Mechanics, Technische Universität München, Boltzmannstraße 15, 85747 Garching b. München, Germany

E-mail: hammerl@lnm.mw.tum.de

Abstract. An Euler-Lagrange model is developed to simulate bubbly flow around an obstacle with the aim to resolve large and meso-scales of cavitation phenomena. The volume averaged Navier-Stokes equations are discretized using finite elements on an unstructured grid with a variational multiscale method. The trajectory of each bubble is tracked using Newton's second law. Furthermore, bubble interaction is modeled with a soft sphere contact model to obtain a four-way coupled approach. The new features presented in this work, besides using a variational multiscale method in an Euler-Lagrange framework, is an improved computation of the void fraction. A second order polynomial is used as filtering function and the volume integral is transformed by applying the divergence theorem twice, leading to line integrals which can be integrated analytically. Therefore, accuracy of void fraction computation is increased and discontinuities are avoided as is the case when the kernel touches a Gauss point across time steps. This integration technique is not limited to the chosen spatial discretization. The numerical test case considers flow in a channel with a cylindrical obstacle. Bubbles are released close to the inflow boundary and void fractions up to 30 % occur at the stagnation point of the obstacle.

1. Introduction

Cavitation is a very important phenomenon that can be highly detrimental, e.g. when occurring at ship propellers. Vapor bubbles, formed within the fluid phase due to a sudden drop of local pressure, can cause structural damage when collapsing or lead to power loss. Millions of small nuclei, which can be found in any liquid, strongly influence cavitation inception. Simplified approaches to simulate cavitation include homogeneous flow models with a proper equation of state or two-fluid Eulerian approaches considering the volume fractions of each phase. However, due to the recent developments in computational resources and methods, it becomes feasible to simulate each nucleus as a particle which is tracked throughout a simulation in the scope of an Euler–Lagrange model.

2. Numerical Model

The liquid phase is described by the volume-averaged incompressible Navier-Stokes equations. The continuity equation is reformulated as in [1] leading to a non-divergence free fluid field:

$$\nabla \cdot \mathbf{u} = -\frac{1}{\epsilon_l}\left(\frac{\partial \epsilon_l}{\partial t} + \mathbf{u} \cdot \nabla \epsilon_l\right) \tag{1}$$

where ϵ_l denotes the liquid-phase volume fraction and $\mathbf{u}$ is the volume averaged fluid-phase velocity. Following [7], the volume averaging procedure reads

$$\epsilon_l \rho_l \frac{\partial \mathbf{u}}{\partial t} + \epsilon_l \rho_l \mathbf{u} \cdot \nabla \mathbf{u} = -\nabla p + \nabla \cdot \boldsymbol{\tau} + \epsilon_l \rho_l \mathbf{g} + \mathbf{s} \tag{2}$$

using the pressure p, the temporal and spatial constant liquid-phase density ρ_l and the viscous stress tensor $\boldsymbol{\tau} = \mu \left((\nabla \mathbf{u}) + (\nabla \mathbf{u})^T \right) - \frac{2}{3} \mu (\nabla \cdot \mathbf{u}) \mathbf{I}$ with the dynamic viscosity μ and the identity tensor $\mathbf{I}$. The gravity vector and the coupling term with the bubbles are denoted by $\mathbf{g}$ and $\mathbf{s}$, respectively.

The fluid is described in an Eulerian frame whereas the bubbles are handled as discrete points which are tracked individually in a Lagrangian frame using Newton's second law:

$$m_b \frac{\mathrm{d}}{\mathrm{d}t} \dot{\mathbf{v}} = \mathbf{F}_G + \underbrace{\underbrace{\mathbf{F}_D + \mathbf{F}_L + \mathbf{F}_{VM}}_{=-\mathbf{s}'} + \mathbf{F}_P + \mathbf{F}_{VISC}}_{=-\mathbf{s}} + \mathbf{F}_C \tag{3}$$

in which m_b and $\mathbf{v}$ are the bubble mass and velocity, respectively. Gravity force, drag force, lift force, virtual mass force, and pressure force are chosen as in [2] using a constant lift and virtual mass coefficient $c_l = c_{vm} = 0.5$. The drag coefficient c_d is adopted from [3]. Viscous forces

$$\mathbf{F}_{VISC} = V_b \nabla \cdot \tau \tag{4}$$

of a bubble with volume V_b require the computation of second derivatives of the fluid velocity which are zero for linear finite elements as they are used in this work. Therefore, a reconstruction of the first derivatives using an L2-projection is applied. The collision force is computed using a soft sphere contact model with the normal gap $g_{n,ij}$, unit normal vector $\mathbf{n}_{ij}$ from bubble i to bubble j, and the stiffness parameter k_c according to $\mathbf{F}_C = k_c g_{n,ij} \mathbf{n}_{ij}$ if $g_{n,ij} \leq 0$. Bubble-wall collisions are modeled assuming infinite mass of the wall element. The coupling force $\mathbf{s}$ does not include gravity and collision forces when choosing the momentum equation as in (2). Furthermore, the pressure force and viscous force can be dropped from the coupling term $\mathbf{s}$ when combined with the respective terms in the momentum equation [4]. The coupling term is then denoted as $\mathbf{s}'$ and the momentum equation reads

$$\epsilon_l \rho_l \frac{\partial \mathbf{u}}{\partial t} + \epsilon_l \rho_l \mathbf{u} \cdot \nabla \mathbf{u} = -\epsilon_l \nabla p + \epsilon_l \nabla \cdot \boldsymbol{\tau} + \epsilon_l \rho_l \mathbf{g} + \mathbf{s}' \ . \tag{5}$$

The final formulation of the volume-averaged NS equations used in this work are obtained by dividing (5) by ϵ_l, and the continuity equation as given in (1).

The Euler–Lagrange model is based on a variational multiscale method for the underlying fluid according to [5] and thus it is possible to distribute coupling forces from the bubbles using the shape functions evaluated at the position of the bubble within the element. Hence, a conservative coupling can be achieved because of the partition of unity property of finite element shape functions. Fluid velocity and acceleration are necessary to evaluate the bubble forces. Interpolation from fluid quantities such as velocity and acceleration is also performed using the shape functions evaluated at the bubble position. The computation of the volume fraction occupied by the bubbles cannot be handled by the finite element discretization directly. In order to avoid pulsating velocity fluctuations in the fluid field when assigning the full bubble volume to a single element as described in [6], a remedy are smooth kernel functions with zero tangents at their bounds of influence, see also [6]. This reduces oscillations due to Gaussian

integration. In this work, a distribution using a quadratic filtering function

$$\Psi^d = \begin{cases} \frac{3}{4}\left(-\frac{\left(x^d - x_j^d\right)^2}{\sigma^3} + \frac{1}{\sigma}\right) & \text{, if} \quad -\sigma \leq \left(x^d - x_j^d\right) \leq +\sigma \\ 0 & \text{, else} \end{cases} \tag{6}$$

for direction d around the bubble position x_j^d together with an improved integration of the resulting volume integral is proposed. The radius of influence $\sigma = 1.2\, r_{b,j}$ is chosen to smear the volume fraction across the underlying fluid elements. The volume integral

$$\sum_{i=1}^{n_{bub}} V_{b,i} \int_{\Omega_j} \Psi_i^x \Psi_i^y \Psi_i^z \mathrm{dxdydz} \tag{7}$$

over the domain Ω_j of fluid element j gives its partial volume that is occupied by all n_{bub} bubbles. The bubble influence volume is assumed to be cubic, as proposed in [8], which allows for a special treatment of the volume integral that is usually solved using Gaussian integration. If the fluid elements are distorted and not enough Gauss points are chosen, loss of accuracy in the calculation of the void fraction can occur. Inspired by [9], the volume integral is transformed to line integrals via applying divergence theorem twice instead of using Gaussian integration. The evaluation of the resulting line integrals is as expensive as using four Gauss points in each direction but accuracy is highly increased. This integration scheme allows for an infinite bubble movement to result in an infinite change in void volume which is superior to Gaussian integration.

The fluid flow is solved on an unstructured grid using stabilized linear finite elements with implicit time integration with generalized-α time integration ($\alpha_m = \frac{5}{6}, \alpha_f = \gamma = \frac{2}{3}$) as applied in [5]. Larger time step can be chosen than for the explicit Velocity-Verlet algorithm for the bubbles. Hence, subcycling is applied and one fluid step is followed by 100 bubble steps.

3. Results

The following test case with flow around a cylindrical obstacle is chosen because it can be seen as a simplified geometry of a hydrofoil. The box like geometry of 5.0 m × 2.0 m × 0.4 m (length × height × depth) contains a cylindrical hole in width direction with a diameter of 0.5 m located in the height mid plane in a distance of 1.5 m from the inflow. Fluid inflow from the left is ramped from zero to 1.0 m/s within 0.05 s. This velocity is also prescribed on the top and bottom surface whereas a slip condition is prescribed on the sides in order to model an infinitely extended cylinder. On the outflow on the right a do nothing boundary condition is imposed. Bubble inflow of 2121 bubbles is started at time $t = 0.01$ s and repeated every 0.01 s within the first layer of fluid elements 0.01 m from the inflow. The inflow velocity is chosen equal to the underlying fluid velocity and the inflow position is determined by using a rectangular grid with 101 times 21 grid points in height and width direction, respectively. A random offset of up to 20 % of the bubble radius is added to each initial position to break symmetry. The bubble radius $r_b = 0.004$ m and its density $\rho_b = 0.001$ kg/m^3. The stiffness parameter k_c is set to 0.021 N/m leading to a maximum overlap of less than 0.02 % of the bubble radius. The fluid with dynamic viscosity $\mu = 8.9 \cdot 10^{-4}$ Pa s and density $\rho_l = 1.0$ kg/m^3 is discretized with 53448 tri-linearly interpolated unstructured hexahedral elements without refinement in the near wall region and a time step size of $\Delta t = 0.01$ s. Gravity acceleration is neglected. In Figure 1 (left), the nuclei are depicted and colored with their velocity magnitude at $t = 5.0$ s. The boundary surfaces of the fluid are also included in the figure but the front and rear surface are removed. Vortex shedding is about to start in the wake of the cylindrical obstacle. Due to bubble Reynolds number smaller unity, the bubbles follow the fluid flow quite accurately and can be seen as marker in the fluid flow. The cross section of the channel is reduced at the obstacle position leading to an

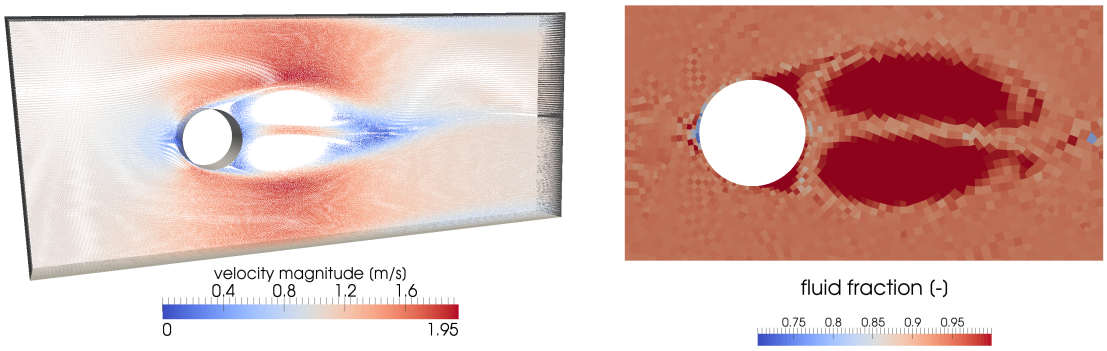

Figure 1. Bubble velocity (left) and close-up of fluid fraction in mid-plane (right) at $t = 5.0$ s.

increased fluid velocity which directly influences the bubble velocity. At the stagnation point of the obstacle bubbles are slowed down and extensive inter-particle contact as well as contact with the cylindrical surface occurs. In this region, fluid fraction goes down to about 70 % as depicted in Figure 1 (right).

4. Summary and Outlook

An Euler–Lagrange model based on a variational multiscale method for the fluid is presented in which bubble movement is driven by Newton's second law. The new feature of this contribution is the usage of the finite element model for the volume averaged Navier-Stokes equations in such a framework and an improved computation of the void fraction which is not limited to the discretization type. The volume integral is transformed into line integrals by applying divergence theorem twice. This obviates Gaussian integration and allows for analytical integration, which is more accurate. Further developments will focus on the investigation of damage due to cavitation. Therefore, the bubble radius, which is assumed constant so far, will be modeled based on the Rayleigh-Plesset equation. Thus, position and time of collapses can be detected dependent on the ambient conditions.

References

[1] Shams E, Finn J and Apte S V 2011 A Numerical Scheme for Euler–Lagrange Simulation of Bubbly Flows in Complex Systems, *Int. J. Numer. Meth. Fluids* **67** 1865–1898
[2] Darmana D , Deen N G, Kuipers J A M 2006 Parallelization of an Euler–Lagrange model using mixed domain decomposition and a mirror domain technique: Application to dispersed gas-liquid two-phase flow *J. Comput. Phys.* **220** 216–248
[3] Deen N G, Van Sint Annaland M, Van der Hoef M A and Kuipers J A M 2007 Review of discrete particle modeling of fluidized beds *Chem. Eng. Sci.* **62** 28–44
[4] Di Renzo A and Di Maio F P 2007 Homogeneous and bubbling fluidization regimes in DEM–CFD simulations: Hydrodynamic stability of gas and liquid fluidized beds *Chem. Eng. Sci.* **63** 116–130
[5] Gravemeier V, Kronbichler M, Gee M W and Wall W A 2011 An algebraic variational multiscale-multigrid method for large-eddy simulation: generalized- time integration, Fourier analysis and application to turbulent flow past a square-section cylinder *Comput. Mech.* **47** 217–233
[6] Kitagawa A, Murai Y and Yamamoto F 2001 Two-way coupling of Eulerian–Lagrangian model for dispersed multiphase flows using filtering functions *Int. J. Multiphase Flow* **27** 2129–2153
[7] Crowe C T, Schwarzkopf J D, Sommerfeld M and Tsuji Y 2012 Multiphase Flows with Droplets and Particles (CRC Press)
[8] Tomiyama A, Zun I, Higaki H , Makino Y and Sakaguchi T 1997 A three-dimensional particle tracking method for bubbly flow simulation *Nuclear Engineering and Design* **175** 77–86
[9] Sudhakar Y and Wall W A 2013 Quadrature schemes for arbitrary convex/concave volumes and integration of weak form in enriched partition of unity methods *Comput. Methods Appl. Mech. Engrg* **258** 39–54